Long-Lasting GABA-Mediated Depolarization Evoked by High-Frequency Stimulation in Pyramidal Neurons of Rat Hippocampal Slice Is Attributable to a Network-Driven, Bicarbonate-Dependent K$^+$ Transient

Kai Kaila, Karri Lamsa, Sergei Smirnov, Tomi Taira, and Juha Voipio

Department of Biosciences, Division of Animal Physiology, University of Helsinki, FIN-00014 Helsinki, Finland

Biphasic GABA$_A$-mediated postsynaptic responses can be readily evoked in CA1 pyramidal neurons of rat hippocampal slices by high-frequency stimulus (HFS) trains in the presence of ionotropic glutamate receptor antagonists. In the present experiments with sharp microelectrodes, whole-cell techniques, and K$^+$-selective microelectrodes, an HFS train (40 pulses at 100 Hz) applied in stratum radiatum close to the recording site evoked a brief hyperpolarizing IPSP (hIPSP), which turned into a prolonged (2–3 sec) depolarization (GABA-mediated depolarizing postsynaptic potential; GDPSP). The *I–V* relationships of the postsynaptic currents (hIPSC and GDPSC) had distinct characteristics: the hIPSC and the early GDPSC showed outward rectification, whereas the late GDPSC was reduced with positive voltage steps to zero or beyond (inward rectification), but often no clear reversal was seen. That two distinct currents contribute to the generation of the GDPSP was also evident from the finding that a second HFS train at peak or late GDPSP induced a prompt GABA$_A$-mediated hyperpolarization. The GDPSP/C was dependent on the availability of bicarbonate, but not on interstitial or intrapyramidal carbonic anhydrase activity.

The HFS train evoked a rapid GABA$_A$-mediated bicarbonate-dependent increase in the extracellular K$^+$ concentration ([K$^+$]$_o$), and the GDPSP followed the K$^+$ transient in a sub-Nernstian manner. The spatial and pharmacological characteristics of the [K$^+$]$_o$ shift indicated that it is generated by a local network of GABAergic interneurons. The brief ascending phase of the GDPSP is linked to a K$^+$-dependent accumulation of intracellular Cl$^-$. Thereafter, a nonsynaptic mechanism, a direct depolarizing effect of the [K$^+$]$_o$ shift, is responsible for the most conspicuous characteristics of the GDPSP: its large amplitude and prolonged duration.

Key words: GABA$_A$ receptor; postsynaptic depolarization; bicarbonate; potassium; hippocampal pyramidal neuron; inhibitory network; glial depolarization

Fast inhibitory GABA$_A$ receptor-mediated postsynaptic potentials (fIPSPs) evoked by single stimuli in hippocampal pyramidal neurons are strongly hyperpolarizing, with a reversal potential ~15–20 mV more negative than the resting membrane potential (for references, see Nicoll et al., 1990). This is consistent with the presence of a powerful Cl$^-$-extruding mechanism (most likely a K$^+$–Cl$^-$ cotransporter) in pyramidal neurons (Thompson and Gähwiler, 1989a; Jensen et al., 1993) (for review, see Kaila, 1994; Payne et al., 1996). However, a biphasic postsynaptic response that also is mediated by GABA and that consists of an initial hyperpolarizing IPSP (hIPSP), followed by a slow depolarization, can be readily evoked in hippocampal pyramidal neurons by high-frequency stimulation of inhibitory interneurons in the presence of ionotropic glutamate receptor antagonists (Davies and Collingridge, 1993; Grover et al., 1993; Staley et al., 1995). Because the amplitude of the slow depolarization is often sufficient to elicit spike firing, which by definition means that this response is excitatory rather than inhibitory, we prefer calling it a GABA-mediated depolarizing postsynaptic potential (GDPSP) rather than a "depolarizing IPSP" (cf. Grover et al., 1993).

The ionic mechanism of generation of the GDPSP has been a long-lasting and well recognized enigma (Nicoll et al., 1990; Kaila, 1994; Lambert and Grover, 1995). It has been suggested recently (Staley et al., 1995) that this GABA$_A$ receptor-mediated excitatory response is the result of an asymmetric, activity-dependent collapse of the opposing electrochemical gradients of the two anions (chloride and bicarbonate) that are permeant across GABA$_A$ receptors (Bormann et al., 1987; Kaila and Voipio, 1987). According to the scheme of Staley et al. (1995), the bicarbonate current generated during intense activation of GABA$_A$ receptors in a pyramidal neuron leads to a large depolarization-driven gain in postsynaptic Cl$^-$. There is only a modest net loss of postsynaptic HCO$_3^-$, because the latter is thought to be replenished effectively by the action of both an interstitial (cf. Kaila et al., 1992) and intrapyramidal (cf. Pasternack et al., 1993) carbonic anhydrase. This kind of a mechanism has its precedent in work on crayfish muscle fibers, in which direct measurements of the two anions showed that tonic activation of GABA$_A$ receptor channels can lead to a HCO$_3^-$-dependent depolarization and to a consequent channel-mediated accumulation of intracellular Cl$^-$ (Kaila and Voipio, 1987; Kaila et al., 1989).

The present study supports a key role for HCO$_3^-$ ions in GABAergic depolarization of CA1 pyramidal neurons in rat hippocampal slices. However, our observations indicate that a postsynaptic bicarbonate current in the pyramidal neuron cannot account for the two characteristic properties of the GDPSP, its

extremely positive reversal potential and its prolonged duration. A hypothesis consistent with presently available data (see also Lamsa and Kaila, 1997) is based on a mechanism with a dual role for an activity-induced extracellular K^+ ($[K^+]_o$) transient that is generated in an HCO_3^--dependent manner by a local inhibitory network. The initial fast positive shift in the reversal potential of the relatively short-lived $GABA_A$ receptor-mediated current evoked by a high-frequency stimulus (HFS) train is linked to a postsynaptic accumulation of Cl^- in response to the $[K^+]_o$ transient. Thereafter, a direct depolarizing action of the $[K^+]_o$ shift governs the behavior of the GDPSP.

Some preliminary findings have been published in abstract form (Kaila et al., 1995; Voipio et al., 1996).

MATERIALS AND METHODS

Slice preparation and maintenance. Hippocampal slices (400 μm) were prepared as described elsewhere (Voipio et al., 1995) from brains of 30- to 45-d-old male Wistar rats (100–120 gm). The standard physiological solution that was used contained (in mM): NaCl 124, KCl 3.0, $CaCl_2$ 2.0, $NaHCO_3$ 25, NaH_2PO_4 1.1, $MgSO_4$ 2.0, and D-glucose 10. It was gassed continuously with 95% O_2/5% CO_2, pH 7.4, at the experimental temperature of 32°C. The slices were allowed to recover for ~1 hr at room temperature before being placed into the interface-type recording chamber. In some experiments $NaHCO_3$ was replaced by 20 mM HEPES, pH 7.4 with NaOH, and the solution was equilibrated with 100% O_2.

Stimulation and recording. Synaptic responses in CA1 pyramidal neurons were evoked by stimuli (20 V for 50–100 μsec) delivered with a bipolar electrode placed in stratum radiatum at a distance of ~0.5 mm from the site of recording. The standard high-frequency train of stimuli consisted of 40 pulses delivered at 100 Hz; occasionally, 100 pulses were applied at 200 Hz. Single stimuli usually were given at a rate of <0.05 Hz and in some experiments at 0.5 Hz (compare Fig. 7).

Intracellular recordings from CA1 pyramidal neurons were obtained by using sharp microelectrodes or patch pipettes. The sharp microelectrodes were filled with a solution containing 1.5 M K-acetate, 1.5 M K-methane sulfonate, and 5 mM KCl, pH 6.8–7.0. They had a resistance of 80–120 MΩ and were used for recording in bridge mode. Only cells with a stable membrane potential of −60 to −75 mV and an input impedance of 20–80 MΩ were used for measurements.

Whole-cell recordings were obtained by using the method of Blanton et al. (1989). An Axoclamp 2A amplifier (Axon Instruments, Foster City, CA) was used either in continuous voltage-clamp mode or in bridge mode. The whole-cell patch pipettes had a resistance of 6–9 MΩ when filled with a solution containing (in mM): K-gluconate 120, $MgCl_2$ 2.0, Mg-ATP 5.0, HEPES 10, K-BAPTA or K-EGTA 2, and D-glucose 20, pH 7.1 with NaOH. The input impedance during the temporary "on-cell" configuration exceeded 1 GΩ, and, immediately after rupturing of the membrane, the membrane potential was usually −45 to −50 mV and cell impedance was 80–100 MΩ. Within 5 min these parameters stabilized at a level of −50 to −70 mV and 100–500 MΩ (typically 150–200 MΩ), respectively.

K^+-selective microelectrodes with a short column of the ion sensor (Fluka 60938, Buchs, Switzerland) were made from double-barreled borosilicate glass pipettes, using techniques described before (Voipio et al., 1995). The reference barrel was filled with 150 mM NaCl. The resistance of the two barrels was 10–20 GΩ and 10–20 MΩ. The electrode responses were calibrated in terms of free concentration, and they had a slope of 56–59 mV for a 10-fold change in $[K^+]$.

Drugs. All experiments (except for those related to Fig. 8*A*) were made in the presence of ionotropic glutamate receptor antagonists, 10 μM 6-nitro-7-sulfamoylbenzo(f)-quinoxaline-2,3-dione (NBQX), 40 μM D-2-amino-5-phosphonopentoate (AP5), and 50 μM ketamine. Picrotoxin was applied in some experiments at a concentration of 100 μM. In most experiments $GABA_B$ receptors were blocked with bath-applied 200 μM CGP 35348 (kindly donated by Dr. M. Pozza, Ciba-Geigy, Basel, Switzerland), by 200 μM 2-hydroxy-saclofen, and/or by the addition of 50–100 μM QX-314 into the whole-cell electrode filling solution. A few experiments were performed with bath-applied atropine (5 μM) or eserine (5–10 μM). Benzolamide (BA), a poorly permeant inhibitor of carbonic anhydrase, either was applied in the bath (10 μM) or was perfused intracellularly (100 μM), using the whole-cell recording electrode. Ethoxyzolamide (EZA), a membrane-permeant carbonic anhydrase in-
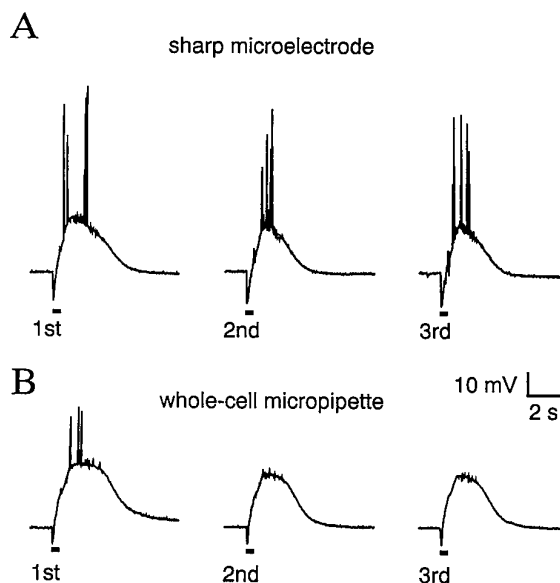

Figure 1. Postsynaptic voltage responses evoked by the standard HFS train (40 pulses at 100 Hz) in the presence of ionotropic glutamate receptors. The first three responses from two cells recorded with a sharp microelectrode or a whole-cell micropipette are shown. Note the somewhat more pronounced depolarization evoked by the first HFS train. In this and subsequent figures, the timing of the HFS train (40 pulses at 100 Hz) is indicated by a *horizontal bar*.

hibitor, was applied at 50 μM in the bathing solution. BA was obtained as a gift from Lederle Laboratories (American Cyanamid, Washington, DC), and EZA was a gift by Professor Gerolf Gros (University of Hannover, Hannover, Germany). NBQX and AP5 were obtained from Tocris Cookson (Bristol, UK). All other chemicals were obtained from Sigma (St. Louis, MO).

Below, data are given as mean ± SEM, if not stated otherwise.

RESULTS

Characterization of postsynaptic responses

Postsynaptic potentials

In agreement with previous results obtained in the presence of ionotropic glutamate antagonists (Grover et al., 1993; Staley et al., 1995), the standard HFS train (40 pulses at 100 Hz) applied to the s. radiatum close to the intracellular recording site evoked a fused sequence of initially hyperpolarizing fast IPSPs (fIPSPs). As seen in recordings obtained with both sharp microelectrodes and whole-cell pipettes (Fig. 1*A,B*), the hyperpolarizing phase of the fused response (to be called the hIPSP) reached its peak amplitude of approximately −10 mV usually within ~30–50 msec and thereafter turned promptly (within 200–300 msec; see Table 1) into a prolonged depolarization (the GDPSP) that often had an amplitude sufficient to trigger a burst of action potentials. Qualitatively similar responses were seen when 100 pulses were given at 200 Hz, which resulted in a slightly larger depolarizing response and somewhat more intense spiking (data not shown). All of the statistics given below are from responses to the standard 40 pulse/100 Hz train.

A prominent feature of the GDPSP evoked in the present manner is that its duration is much longer than the period of stimulation. For reasons not clear at present, we found that the first GDPSP evoked in any given slice consistently had an amplitude and a duration that exceeded by 15–25% those elicited later. After the first response, the GDPSP stabilized at a more constant level when the trains of stimuli were applied at intervals of 3–5

Table 1. Characteristics of the postsynaptic responses

	hIPSP		Time to reversal of polarity (msec)	GDPSP		
	Amplitude (mV)	Time[a] to peak (msec)		Amplitude (mV)	Time to peak (sec)	Half-decay (sec)
Sharp microelectrode	10.8 ± 0.6 ($n = 53$)	36 ± 3 ($n = 53$)	232 ± 12 ($n = 53$)	20.2 ± 0.6 ($n = 46$)	1.29 ± 0.05 ($n = 46$)	2.85 ± 0.10 ($n = 46$)
Whole-cell micropipette	9.9 ± 0.5 ($n = 55$)	44 ± 3 ($n = 55$)	286 ± 18 ($n = 55$)	17.5 ± 0.5 ($n = 47$)	1.50 ± 0.05 ($n = 47$)	2.95 ± 0.09 ($n = 47$)

	hIPSC[b]	Time to reversal of current (msec)	GDPSC[b]	
	Time to peak (msec)		Time to peak (sec)	Half-decay (sec)
Whole-cell micropipette	51 ± 3 ($n = 37$)	277 ± 20 ($n = 37$)	1.11 ± 0.04 ($n = 31$)	2.29 ± 0.08 ($n = 31$)

[a] All values for time courses refer to onset of HFS train.
[b] Data obtained from measurements at resting membrane potential.

min. Hence, the first response was omitted from all quantitative measurements and illustrations except for Figure 1, *A* and *B*. However, during lengthy experiments some "run-down" of the GDPSP often was evident, which usually involved a decrease in its duration rather than in the amplitude.

We found no clear differences in the amplitude of GDPSPs recorded with sharp microelectrodes and whole-cell pipettes, but the time course of the response seemed to be somewhat slower in whole-cell recordings (see Table 1). The GDPSP reached its peak amplitude of ~15–20 mV with a delay of 1.0–1.5 sec as measured from the onset of the stimulus train, and the decay to 50% of maximum amplitude took place at ~3 sec. Both the hIPSP and the GDPSP were abolished by the $GABA_A$ receptor antagonist picrotoxin, with the GDPSP showing a higher sensitivity to this blocker (data not shown; see Grover et al., 1993; Taira et al., 1997).

Application of the $GABA_B$ antagonists CGP 35348 (200 μM) or 2-hydroxy-saclofen (200 μM) did not have a major influence on the biphasic postsynaptic response, and only a slight enhancement of both the duration and amplitude of the GDPSP usually was seen (cf. Grover et al., 1993). Nevertheless, all quantitative data and specimen recordings shown in the illustrations were obtained in the presence of bath-applied $GABA_B$ antagonists (see Materials and Methods). In addition, the whole-cell pipette solution usually contained QX-314 (50–100 μM), known to block both postsynaptic spiking and $GABA_B$ receptors (Nathan et al., 1990).

Because, under certain experimental conditions, synaptic responses evoked in CA1 pyramidal neurons can include a prominent component mediated by muscarinic receptors (Cole and Nicoll, 1984), we examined the effects of bath-applied atropine (5 μM) and eserine (5–10 μM). However, neither drug had any discernible effect on the GDPSP.

Postsynaptic currents

In whole-cell voltage-clamp experiments, the current (hIPSC) that corresponded to the hIPSP was outwardly directed and showed rapid fading (Fig. 2*A*). In cells clamped at their resting membrane potential, a reversal of the polarity of the current took place at ~290 msec after the onset of stimulation (see Table 1). The peak of the hIPSC had a reversal potential of -74.2 ± 1.4

mV ($n = 19$). The peak amplitude of the hIPSP/C evidently was affected by the fast anionic redistribution that takes place during repetitive stimulation (see below), because the reversal potential of the hIPSC was less negative than that of single pulse-evoked fIPSCs, which reversed at -79.5 ± 1.2 mV ($n = 49$).

The hIPSC was followed by a current (to be called GDPSC) that was inwardly directed at resting membrane potential. In comparison to GDPSPs recorded with whole-cell pipettes, the GDPSC had a significantly faster time course, with an average time to peak (from the onset of the HFS train) of 1.11 sec and a time to 50% decay of 2.29 sec (see Table 1).

Preliminary examinations of the *I–V* relationships of the GDPSC revealed initially a surprising amount of variation within a single set of recordings, which turned out to be attributable to slight changes in the time point selected for the analysis. Hence, we made *I–V* plots at intervals of 100–200 msec, which revealed a consistent time dependence of the *I–V* characteristics.

As shown in Figure 2*B*, the *I–V* curves of the hIPSC and the early (high-conductance) phase of the GDPSC showed outward rectification at positive holding potentials; significantly, there was a prompt shift of the consecutive *I–V* curves taken at 200 msec intervals, which yielded more positive values for the GDPSC reversal potential as a function of time (Fig. 2*C*).

The *I–V* behavior of the late (low-conductance) phase of the GDPSC was intriguing because not only was the current progressively reduced with positive voltage steps, but very often no clear reversal was seen even at voltages close to zero or beyond (sometimes up to +15 mV). Inward rectification of this kind is opposite to what is expected from a $GABA_A$ receptor-mediated current (for references, see Kaila, 1994). Hence, it was of much interest that a similar type of "asymptotic" behavior at positive voltages was also typical for *I–V* curves related to glial depolarizations evoked by stimulation-induced $[K^+]_o$ transients that took place at the site of recording under the present experimental conditions (see below and Fig. 11).

Because of the time-dependent properties of the GDPSC, it was difficult to select a single unique parameter for its quantitative characterization. A parameter with some physiological relevance is, perhaps, the reversal potential obtained at the instant at which
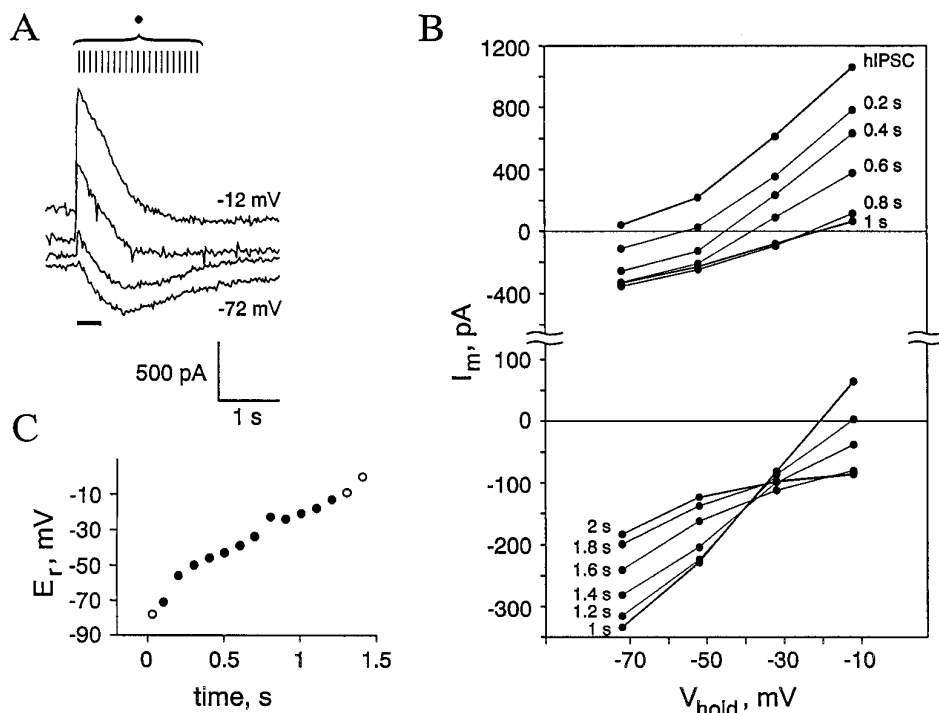
Figure 2. Properties of postsynaptic current responses evoked by the standard HFS train under voltage-clamp conditions. *A,* Specimen recordings of currents. *Vertical bars* indicate the timing of *I–V* samples. *B,* Consecutive *I–V* curves taken at 0.2 sec intervals from the family of recordings in *A,* with the onset of the HFS train assigned time *0.* To facilitate visual inspection, the curves related to 0–1.0 sec (*top panel*) and 1.0–2.0 sec (*bottom panel*) are given separately, with a different scale for current amplitudes. *C,* Change in the reversal potential of the hIPSC/GDPSC as a function of time sampled at 0.1 sec intervals (*open symbols* represent extrapolated values; see *B*). Note that from 1.5 to 2.0 sec, the *I–V* slope is too shallow to yield a meaningful extrapolation.

the GDPSC attains its maximum value when recorded at the resting potential. This gave a mean of -28 mV (range from -22 to -43 mV; $n = 18$) in the present experiments.

Relationships between postsynaptic conductance and voltage responses

In line with the voltage-clamp data, simultaneous measurements of the postsynaptic voltage responses and of the parallel changes in input conductance (Fig. 3) showed that the maximum increase in conductance coincided with the hIPSP, and the conductance fell rapidly to attain a value as low as $26 \pm 4\%$ ($n = 9$) of its maximum at the time of the peak GDPSP. The recovery of the conductance to its resting value was 90% complete at a time when the GDPSP had decayed to only $86 \pm 4\%$ from its maximum.

To examine further the temporal relationships between the voltage and conductance changes associated with GDPSPs, we made experiments in which a second HFS train was applied with variable delays from the first. As shown in Figure 4, this resulted in a hyperpolarization that attained its maximum amplitude when evoked at the peak or late phase of the original GDPSP. With briefer delays, the hyperpolarizing effect of the second train was smaller. However, it is worth stressing that, in all five experiments of this kind, the depolarization during the initial phase of the GDPSP was slowed down markedly by the second train.

It is obvious that if the GDPSP were generated solely by a current across $GABA_A$ receptors under conditions of altered anion gradients, one would expect an enhanced depolarization, rather than a hyperpolarization, in response to further activation of the same synaptic inputs. The above findings indicate that, right after the HFS train, the membrane potential is close to (but slightly more positive than) E_{GABA-A}, but at peak and late GDPSP a level significantly more positive is attained. The evidence to be presented below suggests that the long-lasting depolarization is attributable to an activity-induced network-driven $[K^+]_o$ transient.
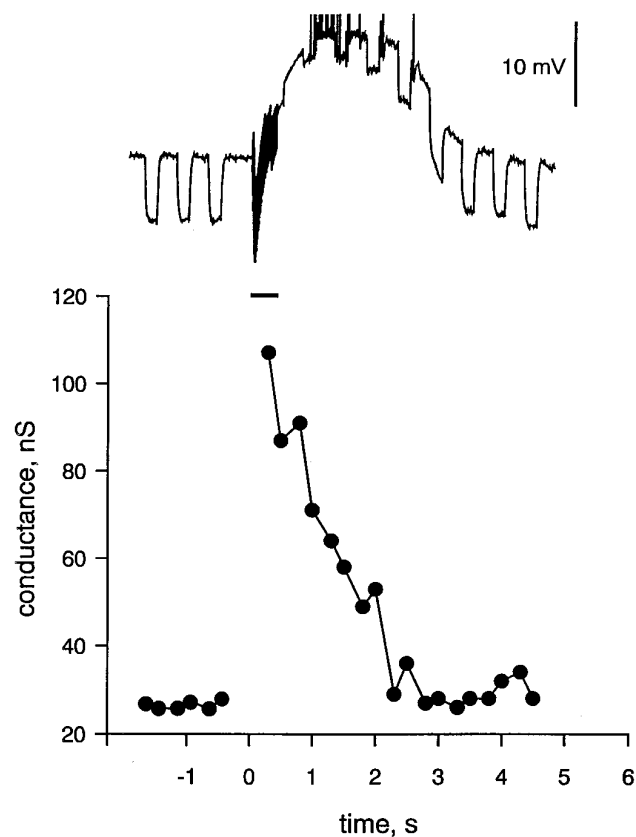

Figure 3. Temporal relationship between the GDPSP and the associated increase in input conductance. There is a rapid decrease in conductance that starts immediately after the onset of the GDPSP and declines almost to its resting level, whereas the GDPSP amplitude is still ~75% of maximum (current–pulse amplitude, -200 pA.)
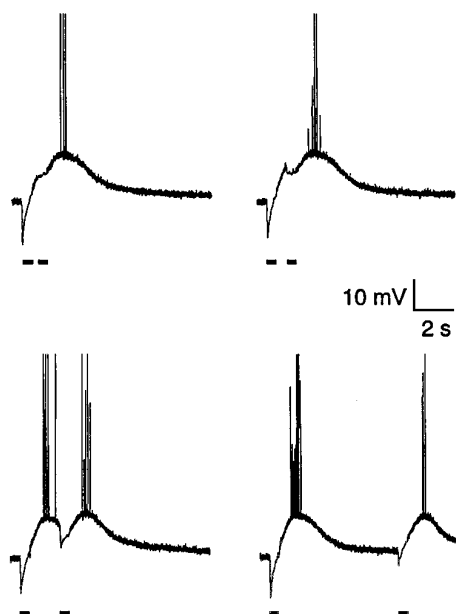
Figure 4. The postsynaptic voltage response to two HFS trains is affected by the timing of the second train. Note that the second train applied during the initial phase of the GDPSP leads to a slowing down of the depolarization, whereas the second train given while the GDPSP is at its peak or decaying phase induces a rapid hyperpolarization.

The GDPSP/C is suppressed in a CO_2/HCO_3^--free medium

After a 30–60 min application of a nominally CO_2/HCO_3^--free (HEPES-buffered) solution with 100% O_2 as the gas phase in the interface chamber, the GDPSP was strongly attenuated, to 10–50% ($n = 4$) of the control response (Fig. 5A). This observation is consistent with a role for HCO_3^- in the generation of the depolarizing response. That a full block was not always seen (compare *top traces* in Fig. 5A) may be attributable at least partly to production of CO_2 (Voipio and Kaila, 1993).

In the absence of HCO_3^-, fading of the hIPSC was strongly slowed down, resulting in voltages close to the resting potential in prolonged outwardly directed currents (Fig. 5B). There was a strong suppression (to $28 \pm 7\%$; $n = 4$) of the GDPSC recorded at resting potential, and the apparent reversal potential (see above) of the peak GDPSC was -60.5 ± 1.3 mV ($n = 4$). All of the effects of the CO_2/HCO_3^--free medium were reversible (data not shown).

Experiments with single stimuli applied at 0.5 Hz showed that the absence of CO_2/HCO_3^- did not have a consistent decremental effect on $GABA_A$ receptor-mediated transmission (compare Fig. 7). The above voltage-clamp experiments also clearly show that the inhibition of the GDPSP in the absence of CO_2/HCO_3^- cannot be explained on the basis of a decrease in presynaptic excitability or a decrease in the input resistance (R_{in}) of the pyramidal neuron (cf. Grover et al., 1993). However, it is of interest to note here that, whereas a decrease in R_{in} of ~15% was observed in sharp microelectrode recordings after withdrawal of CO_2/HCO_3^-, the opposite was true for whole-cell experiments in which an increase in R_{in} of 10–50% was seen. This implies that the resting conductance that is active under the two recording conditions differs not only in amount but also in the mechanisms involved (cf. Staley et al., 1992).
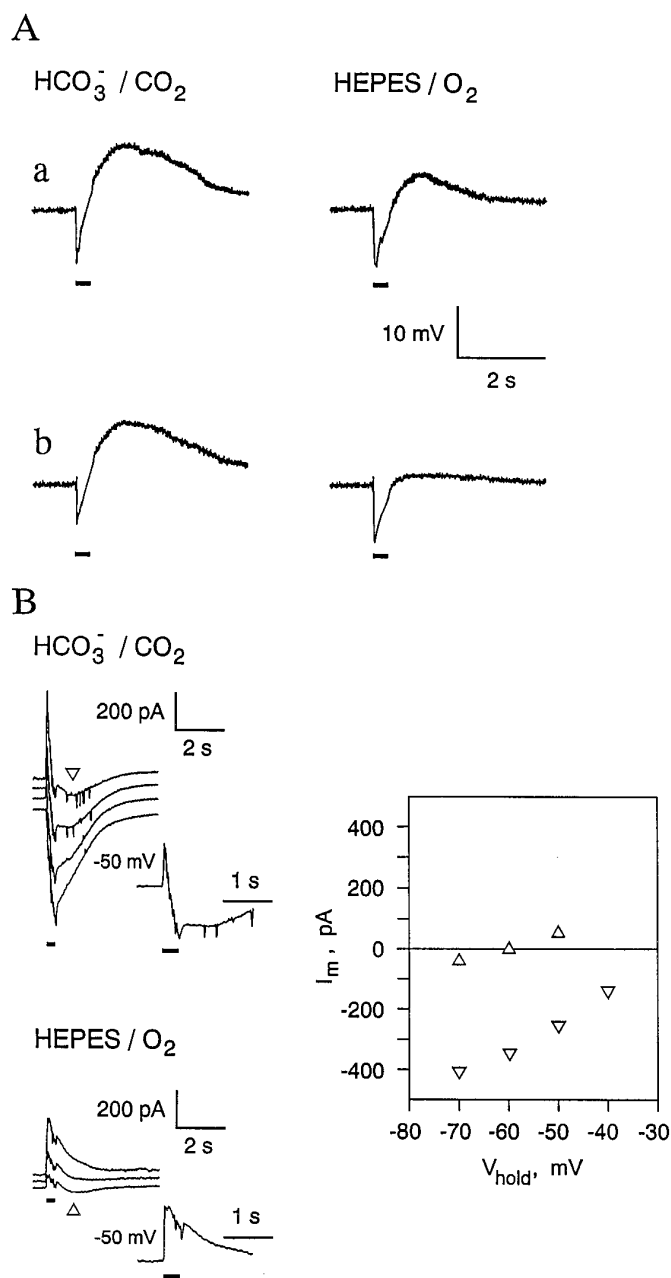

Figure 5. Dependence of GDPSP/C on the presence of CO_2/HCO_3^-. A, The GDPSP is suppressed (cell *a*) or blocked (cell *b*) in a nominally bicarbonate-free solution buffered with HEPES and equilibrated with 100% O_2. B, The GDPSC shows a dependence on bicarbonate similar to the GDPSP. Note that the hIPSC as measured at the resting level of this neuron (-50 mV) is not suppressed in the HEPES/O_2 medium. Recordings at -50 mV are shown at an expanded time scale in both *A* and *B*.

The GDPSP/C is suppressed after global inhibition of intracellular (but not interstitial) carbonic anhydrase

There are functionally distinct kinds of carbonic anhydrases that play a crucial role in activity-induced acid–base shifts in the brain parenchyma: in addition to intracellular isoforms located within certain neurons and glial cells, a distinct one seems to be responsible for rapid CO_2 hydration/dehydration in the interstitial space (Chesler and Kaila, 1992). Therefore, we found it of interest to examine the effects of BA, a poorly permeant carbonic anhydrase inhibitor, and of EZA, a membrane-permeant inhibitor, on the
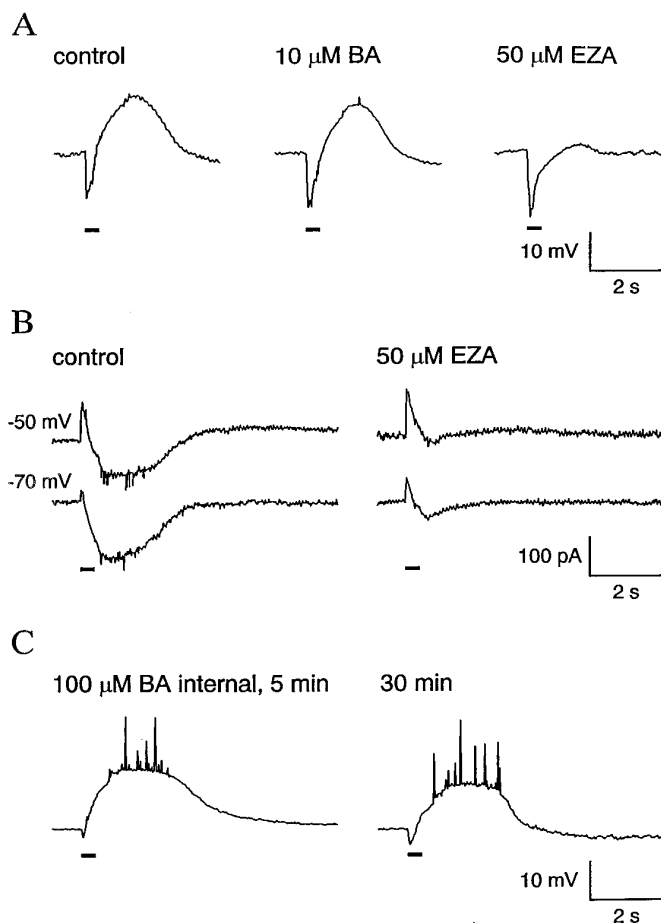
Figure 6. Effects of inhibitors of carbonic anhydrase on the GDPSP/C. *A,* Bath application of the impermeant carbonic anhydrase inhibitor benzolamide (*BA*) has no effect on the GDPSP, whereas a subsequent exposure to the more lipophilic carbonic anhydrase blocker ethoxyzolamide (*EZA*) abolishes the GDPSP. *B,* The GDPSC is inhibited by bath-applied *EZA*. *C,* Intracellular perfusion with *BA* at high concentrations does not block the generation of the GDPSP.

postsynaptic responses (cf. Maren, 1977; Voipio et al., 1995). In nine slices examined, a full block of interstitial carbonic anhydrase with BA (10 μM applied for 30–60 min; Voipio et al., 1995) had no discernible effect on the GDPSP (Fig. 6*A*), whereas a subsequent exposure to 50 μM EZA for 20–40 min produced an attenuation of GDPSP and GDPSC similar to that observed in the absence of CO_2/HCO_3^- (Fig. 6*A,B*).

The above actions of EZA cannot be explained on the basis of a fall in interstitial pH (pH_o) as postulated for the suppressing action of acetazolamide by Grover et al. (1993), because both permeable and impermeable carbonic anhydrase inhibitors have a similar effect on pH_o, producing an extracellular acidosis of ~0.1 pH units (Voipio et al., 1995) (K. Kaila, P. Paalasmaa, and J. Voipio, unpublished results). Even more importantly, the above results show that, in contrast to the model by Staley et al. (1995), the interstitial space does *not* act as a compartment that provides for fast regeneration of the intracellular CO_2/HCO_3^- in the pyramidal neurons. In fact, as shown below, a fast replenishment of intracellular bicarbonate (whatever the source) within the pyramidal neuron is not necessary for the generation of the GDPSP/C.

The GDPSP/C is not blocked by intracellular perfusion of an inhibitor of carbonic anhydrase

Benzolamide is a highly potent drug used to inhibit various carbonic anhydrase isoforms with a concentration for half-maximal inhibition in the nanomolar range (Maren, 1977). In sharp contrast to the obvious prediction of the Staley et al. (1995) model of GDPSP generation, internal perfusion with 100 μM BA (even when applied for 70–80 min; $n = 4$) had no detectable effect on the GDPSP. We also conducted five experiments with sharp microelectrodes containing 10 mM BA in the filling solution, but we failed to see any effect on the GDPSP.

It should be emphasized that the lack of effect on the GDPSP of BA applied intracellularly at concentrations that are at least four orders of magnitude higher than what is needed for complete carbonic anhydrase inhibition is not likely to be attributable to problems of diffusion, because this drug has a molecular weight of only 320, and it is highly soluble in water. Hence, the above results indicate that an action on the pyramidal neuron is not responsible for the inhibition of the GDPSP/C by more lipophilic blockers of carbonic anhydrase inhibitors such as EZA (this study) and acetazolamide (Grover et al., 1993; Staley et al., 1995).

Postsynaptic Cl^- accumulation caused by an electroneutral, bicarbonate-dependent mechanism

It has been demonstrated frequently that repetitive stimulation can lead to a decrease in the amplitude, and even to a change in the polarity, of single pulse-evoked fIPSPs, with no change in synaptic conductance (Wong and Watkins, 1982; Thompson and Gähwiler, 1989b). A widely accepted explanation to account for fIPSP fading and reversal of this kind is a postsynaptic uptake of Cl^- and a consequent positive shift in the reversal potential of the $GABA_A$ receptor-mediated current (Kaila, 1994). To examine the mechanisms of the fast shift in E_{GABA-A} that appears to take place at the initial phase of the GDPSP, we studied the influence of repetitive stimulation on the amplitude and polarity of fIPSCs in five neurons voltage-clamped at the level of their resting membrane potential. Figure 7 shows the results of a such an experiment. Single stimuli applied at a constant rate of 0.5 Hz produced outwardly directed fIPSCs with a constant amplitude. However, interposing a five-pulse train of stimuli at 100 Hz caused a marked (but reversible) suppression of the subsequent fIPSCs, and 10 pulses at 100 Hz caused an immediate (but reversible) change in their polarity. Another important finding in these experiments was that a fast HFS-induced redistribution of Cl^- could not be observed in the absence of HCO_3^-. In the experiment depicted in Figure 7, 5 or 10 pulses applied at 100 Hz in the HEPES-buffered solution had only a small effect on the amplitude of the fIPSCs and did not result in a change in their polarity.

Results of the above kind clearly suggest the presence of an electroneutral mechanism that is able to mediate a remarkably efficient accumulation of postsynaptic Cl^- in response to an HFS train. Of course, this observation does not exclude a significant contribution of a bicarbonate-dependent channel-mediated net influx of Cl^- to the fast positive shift in E_{GABA-A} (cf. Kaila et al., 1989). However, a point worthy of emphasis is that the electroneutral mechanism also shows a dependence on HCO_3^-. Below, we will present evidence for the view that the redistribution of Cl^- is attributable in large part to an HFS-induced bicarbonate-dependent increase in $[K^+]_o$.

HCO_3^- / CO_2

Figure 7. Stimulation-induced reversal of the polarity of fIPSC takes place in a voltage-clamped neuron and is dependent on the presence of HCO_3^-. The cell was clamped at its resting potential, and single stimuli applied at a constant rate of 0.5 Hz produced outwardly directed fIPSCs with a constant amplitude. Interposing a five-pulse train of stimuli at 100 Hz (*5/100 Hz*) in the standard HCO_3^--containing solution caused a suppression of the subsequent fIPSCs, whereas 10 pulses at 100 Hz (*10/100 Hz*) caused a change in their polarity. Similar brief HFS trains had little influence on fIPSCs in the nominally HCO_3^--free HEPES-buffered solution. Data are taken from a continuous recording.
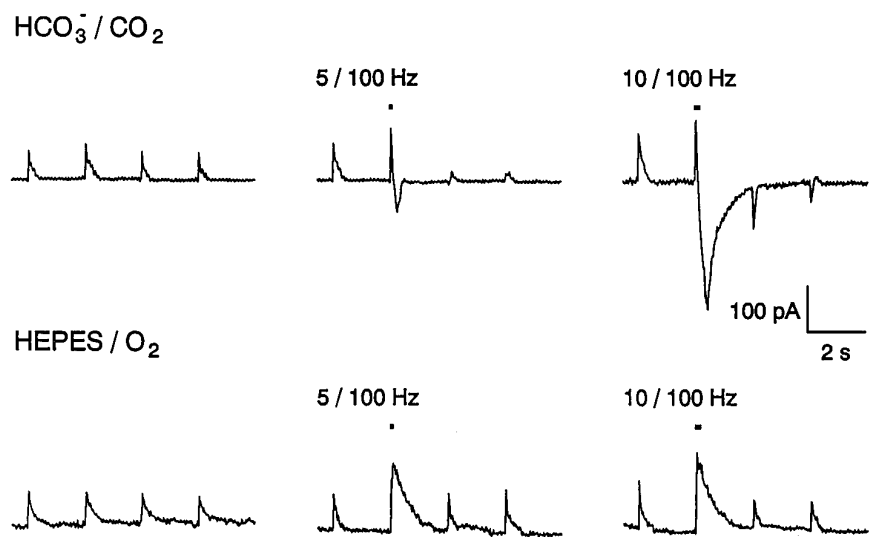
The GDPSP is paralleled by a GABAergic increase in extracellular K^+

The intracellular Cl^- concentration in pyramidal neurons appears to be set by plasmalemmal K^+–Cl^- cotransport (Thompson et al., 1988a,b; Thompson and Gähwiler, 1989a,b; Payne et al., 1996). This makes the reversal potential of $GABA_A$ receptor-mediated currents (E_{GABA-A}) highly sensitive to changes in $[K^+]_o$, with an increase of K^+ leading to a positive shift (Kaila, 1994). Hence, it was of much interest to observe that the GDPSP was tightly linked to a stimulation-induced $[K^+]_o$ transient. The standard HFS train evoked a prompt increase in $[K^+]_o$ in both s. pyramidale and s. radiatum.

Again, all of the experiments on $[K^+]_o$ shifts to be described in more detail were done in the presence of the ionotropic glutamate receptor antagonists. However, it is notable that, with the standard distance between the stimulating and recording electrodes (~500 μm), the application of glutamate antagonists produced only a modest decrease (15–25%; $n = 6$) in the $[K^+]_o$ transient (Fig. 8A), whereas a subsequent application of 100 μM picrotoxin resulted in a near-complete block (data not shown).

Role of HCO_3^- and carbonic anhydrase in the generation of the $[K^+]_o$ transients

Further evidence pointing to the involvement of $[K^+]_o$ transients in GDPSP generation was provided by the identical dependence of the two responses on the presence of CO_2/HCO_3^- and on a functional intracellular carbonic anhydrase activity. As illustrated in Figure 8B, in the HEPES medium the rise in $[K^+]_o$ was much smaller, 30–50% ($n = 5$) of that seen in the control solution. The $[K^+]_o$ transient also was strongly attenuated in the presence of EZA, with a time course of inhibition identical to the effect of the drug on the GDPSP (data not shown). Bath-applied BA had no noticeable effect on the potassium transients.

Spatial and temporal properties of the $[K^+]_o$ transients

The amplitude of the $[K^+]_o$ transient measured in s. radiatum at the standard distance of 500 μm ranged between 2.3 and 4.5 mM ($n = 15$). Simultaneous measurements using two K^+-selective microelectrodes showed that the peak amplitude of the $[K^+]_o$ transient in four of four experiments was slightly larger in s. radiatum (mean increase 3.1 $\pm$ 0.2 mM) than in s. pyramidale (1.9 $\pm$ 0.3 mM). This regional difference is identical to that seen with potassium transients associated with spontaneous GABAer-
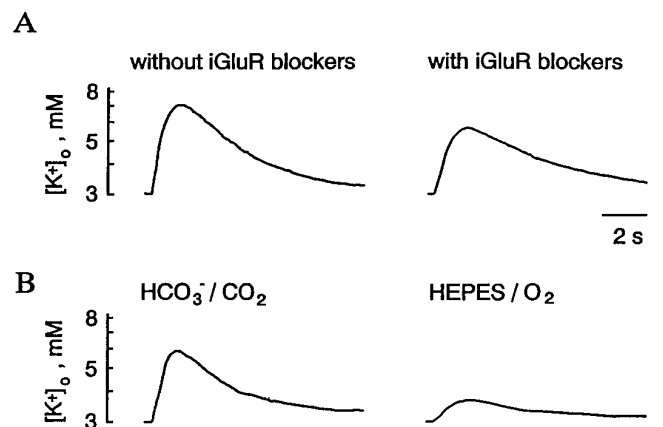

Figure 8. The standard HFS trains evoke large GABAergic bicarbonate-dependent $[K^+]_o$ transients in the CA1 region at the standard distance from the site of stimulation. *A,* The stimulation-induced $[K^+]_o$ transient is affected only slightly by the presence of ionotropic glutamate receptor agonists. (The *left trace* is the only recording shown in the present study that was obtained in the absence of ionotropic glutamate antagonists.) *B,* The stimulation-induced $[K^+]_o$ is suppressed in the absence of CO_2/HCO_3^-.

gic events in slices exposed to 4-aminopyridine (Avoli et al., 1996). The amplitude of the GABAergic K^+ transient decreased steeply as a function of distance from the stimulating electrode, vanishing to zero at a distance of ~1.5–2.0 mm (Fig. 9).

The $[K^+]_o$ transient in s. radiatum had a time to peak of 1.36 $\pm$ 0.32 sec ($n = 15$). Simultaneous intracellular recordings of GDP-SPs and associated $[K^+]_o$ shifts showed that, when evoked by various stimulation frequencies and stimulus train durations, the two responses had a closely matching time course (Fig. 10).

It is also evident from Figure 10 that a similar tight temporal coupling was true for responses involving a second HFS train, such as those examined earlier on (compare Fig. 4). Considering the idea that the $[K^+]_o$ shift is likely to play a significant direct role in the generation of the peak and late phase of the GDPSP (see Discussion), it is notable that in all simultaneous measurements the amplitude of the GDPSP showed a sub-Nernstian behavior with respect to the peak increase in K^+.
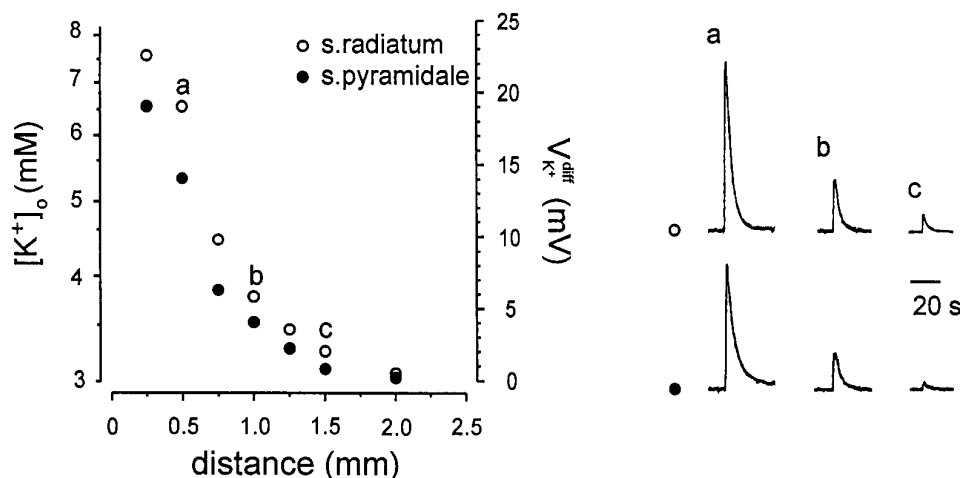
Figure 9. Spatial profile of the activity-induced $[K^+]_o$ shifts. *Left*, the peak amplitude of the $[K^+]_o$ shift is slightly larger in s. radiatum than in s. pyramidale, and it decays steeply as a function of distance from the site of recording. The plot shows peak responses in terms of the absolute level of $[K^+]_o$ attained as well as in terms of the response of the differential signal of the K^+-selective microelectrode (V_{K+}^{diff}). *Right*, Specimen recordings related to data points indicated by *a–c* in the plot.
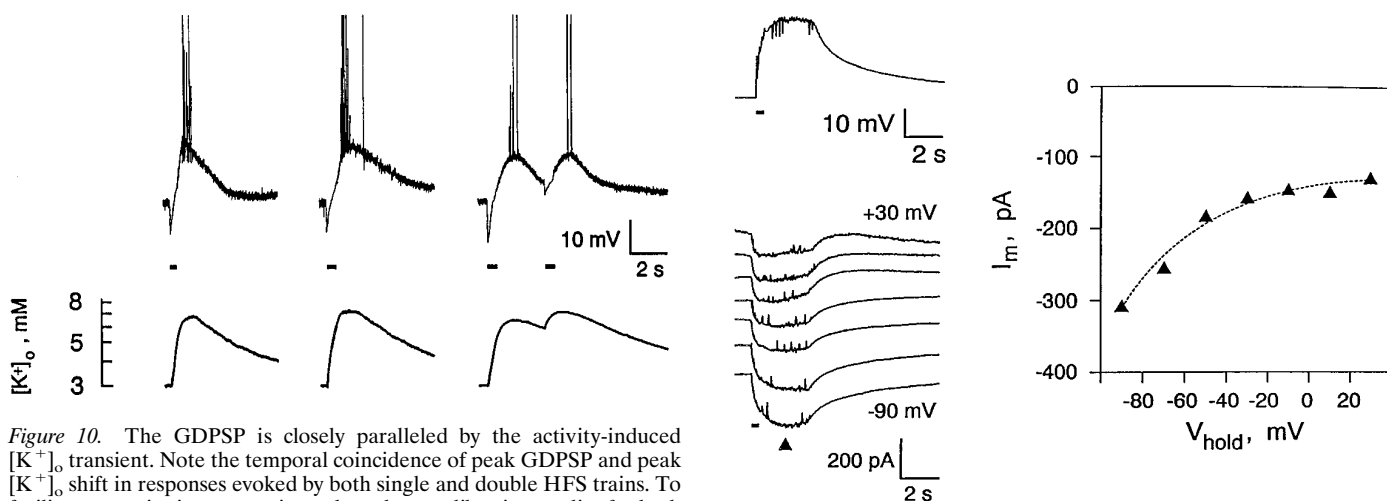

Figure 10. The GDPSP is closely paralleled by the activity-induced $[K^+]_o$ transient. Note the temporal coincidence of peak GDPSP and peak $[K^+]_o$ shift in responses evoked by both single and double HFS trains. To facilitate quantitative comparison, the voltage calibration applies for both the membrane voltage traces (*top traces*) and the K^+ electrode responses (*bottom traces*).

Figure 11. Voltage and current responses evoked by an HFS train in a glial cell under whole-cell recording conditions. The HFS train induces a fast depolarization or an inward current, which shows no tendency for reversal at voltages as positive as +30 mV. The "asymptotic" behavior of the *I–V* plot is what is to be expected from an inward current generated by an activity-induced $[K^+]_o$ transient (*dashed curve* fitted by eye).

Voltage responses and currents generated in glial cells in response to GABAergic $[K^+]_o$ transient

Temporal properties of the glial response

Changes in glial membrane potential have been used frequently to examine activity-induced changes in $[K^+]_o$, because it is known that the plasmalemma of these cells has a high selectivity to K^+ (Lothman and Somjen, 1975). Because the temporal resolution of ion-selective microelectrodes is rather limited (see Voipio et al., 1994), we made intracellular measurements from glial cells to gain further information about the time course of the $[K^+]_o$ shift, especially about its time of onset and rate of rise. The recordings were obtained by using both whole-cell pipettes and sharp microelectrodes from a total of six cells impaled in s. radiatum at the standard distance of ~0.5 mm from the site of stimulation. The cells were identified on the basis of their rather negative membrane potential (−80 to −90 mV) and the absence of any electrogenic response to depolarizing current pulses or to single extracellular stimuli.

The standard HFS train evoked a large depolarization (15–27 mV) in all six of the cells examined (Fig. 11). The responses had a very fast onset, with a delay to 50% of maximum of only 94 ± 9 msec. In view of the temporal properties of the GDPSP/C (see Table 1), it was of interest to note that at the time of the reversal of the hIPSP (~290 msec from the start of the train; see Table 1), the glial membrane potential changes had attained a mean value of 87% of maximum. These data indicate that, at the onset of the GDPSP, $[K^+]_o$ can reach a level of up to 7.4 mM within the interstitial space. As discussed below, such a rise in $[K^+]_o$ will lead to a pronounced inhibition of Cl^- extrusion by K^+–Cl^- cotransport in pyramidal neurons.

I–V relationships of glial current driven by a transient increase in $[K^+]_o$

Figure 11 shows a whole-cell clamp experiment in which glial responses were evoked by the HFS train. As was to be expected from a current generated in response to a transient increase in $[K^+]_o$, the data yielded *I–V* curves with a smooth "asymptotic" behavior, i.e., the inward current was diminished at progressively more positive voltages, but no reversal could be obtained even at voltages as positive as +40 mV. This behavior is qualitatively similar to that of neuronal GDPSCs (see Fig. 2), which agrees with the idea that a direct depolarizing action of the $[K^+]_o$ transient plays an important role in the generation of the GDPSP/C.

DISCUSSION

Experiments on crayfish muscle fibers originally showed that a depolarizing effect mediated by $GABA_A$ receptors does not necessarily imply that Cl^- is actively transported into the postsynaptic cell but that HCO_3^- can act as a carrier of depolarizing current (Kaila and Voipio, 1987; Kaila et al., 1989). A study on neocortical neurons showed that an HCO_3^- versus Cl^- permeability ratio of ~0.2 (cf. Bormann et al., 1987) accounts for a +10 to +15 mV deviation of the reversal potential of $GABA_A$ receptor-mediated fIPSPs from the Cl^- equilibrium potential (E_{Cl}) (Kaila et al., 1993). In view of the fact that all kinds of $GABA_A$ receptors studied to date have an HCO_3^-/Cl^- permeability ratio of ~0.2–0.4 (Kaila, 1994) (see also Fatima-Shad and Barry, 1993), the reversal potential of fIPSPs in hippocampal pyramidal neurons is also likely to be more positive than E_{Cl}. However, it is readily evident from quantitative considerations based on the Goldman–Hodgkin–Katz voltage equation (Hille, 1992) that the extremely positive reversal potential of the GDP-SCs examined presently cannot be explained as an immediate consequence of a HCO_3^- permeability (see Fig. 4 in Kaila and Voipio, 1990).

The apparent paradox above is resolved by the present experiments, which indicate that E_{GABA-A} remains negative with respect to the peak GDPSP, and, as discussed below (Fig. 12), a depolarizing mechanism other than a direct $GABA_A$ receptor-mediated input to the pyramidal neuron has to be involved.

Intrapyramidal and interstitial carbonic anhydrase are not needed for GDPSP/C generation

To explain the biphasic response evoked by tonic activation of $GABA_A$ receptors, Staley et al. (1995) suggested that a large gain of internal Cl^- and a modest net loss of HCO_3^- take place, leading to a fast depolarizing shift in E_{GABA-A}. The inhibitory action of acetazolamide was accounted for by a block of the carbonic anhydrase activity within the pyramidal neuron (cf. Pasternack et al., 1993) and in the interstitial space (cf. Kaila et al., 1992).

The results of the present study do not support a mechanism of the above kind. First, inhibition of interstitial carbonic anhydrase by bath-applied benzolamide did not suppress the GDPSP. Second, there was no suppression of the GDPSP after internal perfusion of the pyramidal neuron with benzolamide. These results indicate that the critical carbonic anhydrase activity that is sensitive to bath-applied EZA (see Fig. 6) is located in an intracellular compartment other than that of the target neuron.

A further finding central to the scheme proposed by Staley et al. (1995) was that amiloride blocked GDPSP generation, an effect thought to be attributable to a fall in the postsynaptic intracellular HCO_3^- in response to a block of Na^+/H^+ exchange. However, the Na^+/H^+ exchanger in pyramidal neurons is known to be *insensitive* to amiloride and its derivatives (Raley-Susman et al., 1993; Schwiening and Boron, 1994; Bevensee et al., 1996). Amiloride is not a specific inhibitor of Na^+/H^+ exchange, and the results obtained by Staley et al. (1995) may well have been caused by a direct effect of the drug on neuronal excitability (cf. Benos, 1982; Tang et al., 1988).

Activity-dependent $[K^+]_o$ transients generated by the GABAergic interneuronal network

An intriguing observation made presently was that large stimulation-induced $[K^+]_o$ transients can be evoked in the CA1 region in the presence of antagonists of ionotropic glutamate
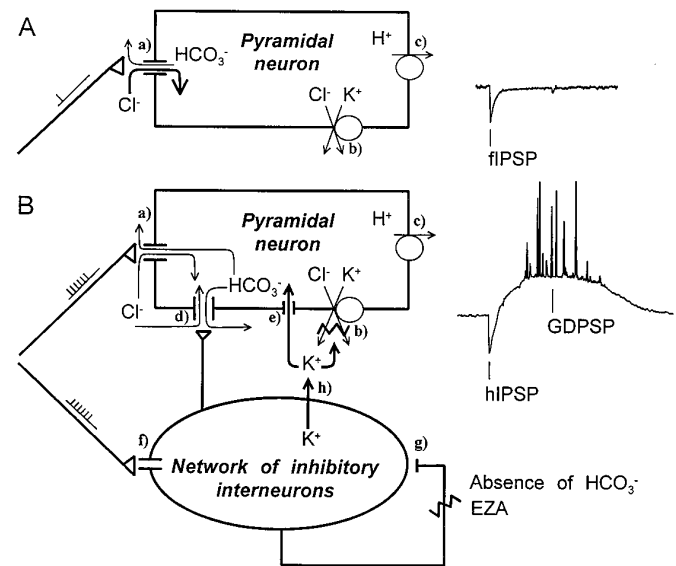

Figure 12. Mechanisms of $GABA_A$ receptor-dependent postsynaptic responses evoked in a pyramidal neuron by a single stimulus (*A*) and by an HFS train (*B*). *A*, Under resting conditions Cl^- is expelled by a $K^+–Cl^-$ cotransporter (*b*), and intracellular HCO_3^- is accumulated by an acid-extruding mechanism (*c*). Because most of the postsynaptic current is carried by Cl^-, the activation of $GABA_A$ receptors by a single stimulus leads to a hyperpolarizing fIPSP. *B*, An HFS train evokes $GABA_A$ receptor-mediated responses in both the pyramidal neuron and the local inhibitory network (*a, f*). The rise in $[K^+]_o$ triggered by the activity of the inhibitory network has two consequences. (1) The increase in $[K^+]_o$ (*h*) inhibits Cl^- extrusion by the $K^+–Cl^-$ cotransporter (*zigzag line*), leading to an accumulation of Cl^- and to a positive shift in E_{GABA-A}, while the $GABA_A$ergic inputs (*a, d*) to the pyramidal neuron are active. This produces the initial phase of the GDPSP that is associated with a large increase in conductance. (2) The $[K^+]_o$ transient outlasts the $GABA_A$ receptor-mediated conductance in the pyramidal cell and has a direct depolarizing action that is mediated by the plasmalemmal K^+ conductance (*e*). The direct depolarizing action of the $[K^+]_o$ transient starts rather soon after the onset of the GDPSP, which leads to a membrane potential that is progressively more positive than E_{GABA-A} (compare with Fig. 4). The present results also indicate that the excitatory coupling within the interneuronal network (*g*) is dependent on the availability of HCO_3^- and is suppressed (*zigzag line*) both in the nominal absence of bicarbonate as well as in the presence of a membrane-permeant inhibitor of carbonic anhydrase (*EZA*).

receptors. The spatial profile (see Fig. 9) and the sensitivity of these $[K^+]_o$ shifts to picrotoxin suggest that they are generated by a local GABAergic interneuronal network.

The conclusion that intense interneuronal activity is capable of producing prominent shifts in $[K^+]_o$ is not a novel one. Experiments on brain slices exposed to the convulsant 4-aminopyridine have demonstrated spontaneous "waves" of GABAergic activity (Aram et al., 1991; Perreault and Avoli, 1992), which are associated with substantial $[K^+]_o$ shifts and with long-lasting neuronal depolarizations (Avoli et al., 1996; Lamsa and Kaila, 1997) (see also Barolet and Morris, 1991).

A withdrawal of CO_2/HCO_3^- as well as the application of a membrane-permeant carbonic anhydrase inhibitor (EZA) led to an attenuation of the HFS-induced $[K^+]_o$ transients (this study) and of spontaneous 4-aminopyridine-induced $[K^+]_o$ shifts (Lamsa and Kaila, 1997). These findings strongly suggest that the mutual $GABA_A$ receptor-mediated excitatory coupling among inhibitory interneurons depends on a functional intracellular CO_2/HCO_3^- buffer. This is also consistent with the observations that a $GABA_A$ receptor-mediated neuronal efflux of HCO_3^- takes

place both in response to HFS in area CA1 (Kaila et al., 1992; Taira et al., 1995; Voipio et al., 1995) and in the presence of 4-aminopyridine-induced spontaneous activity (Lamsa and Kaila, 1997).

Postsynaptic Cl^- accumulation in response to the HFS-induced increase in $[K^+]_o$

Experiments done under voltage-clamp conditions showed that a rather small number of stimuli given at a high frequency are sufficient to produce a large positive shift in E_{GABA-A} (compare Fig. 7). This indicates the presence of a postsynaptic mechanism that leads to an accumulation of Cl^-, which is not driven by the membrane potential. It is likely that, after an HFS train, the activity-induced increase in $[K^+]_o$ results in an inhibition, or reversal, of Cl^- extrusion on postsynaptic $K^+–Cl^-$ cotransport (see Fig. 12; Thompson and Gähwiler, 1989a; Jensen et al., 1993; Payne et al., 1996).

The present results indicate that the HFS train evokes a rise in $[K^+]_o$ up to a level of 8.5 mM, and, at the time of the onset of the GDPSP, $[K^+]_o$ can reach a level of 7.4 mM. Even in the absence of a channel-mediated Cl^- load (see Kaila et al., 1989) and assuming that the 1:1 $K^+–Cl^-$ cotransport mechanism rapidly attains its equilibrium, these $[K^+]_o$ transients can induce an increase in the internal Cl^- concentration from ~4 mM (see Materials and Methods; Kaila et al., 1993) to 10–11 mM. This is sufficient to account for a +16 to +18 mV shift in E_{GABA-A} (cf. Kaila and Voipio, 1990) and for the time-dependent positive shift of the early *I–V* curves that show outward rectification (see Fig. 2*B*).

In a recent paper on hippocampal slices exposed to 4-aminopyridine, Perkins and Wong (1996) have suggested that the late phase of "giant GABA-mediated postsynaptic currents" (GP-SCs) in CA3 pyramidal neurons might be mediated by GABA receptors that are preferentially selective for HCO_3^-. When recorded with pipettes containing a high-Cl^-, low-HCO_3/low pH solution, the late "GABA_D" current was reported to reverse at a more negative level than the initial GABA_A response. However, even when allowing for deviations of the true intracellular anion concentrations from those within the whole-cell electrodes, we have been unable to fit the above observations with *any* anionic permeability ratio. Perhaps more importantly, the "GABA_D" current had a linear *I–V* with a true reversal at approximately −67 mV under standard conditions, which is a far too negative level to explain depolarizations of the kind studied in the present work.

The increase in $[K^+]_o$ has a direct depolarizing action

When a second train of stimuli was applied at the peak of the GDPSP, a prompt hyperpolarization was observed (compare Fig. 4). This provides direct evidence that E_{GABA-A} remains more negative than the membrane potential at the time of maximum depolarization. The nonanionic mechanism that seems to play a crucial role in the generation of the GDPSP is a direct depolarizing action of the HFS-induced $[K^+]_o$ shift. The peak amplitudes of the GDPSPs showed a consistent (but sub-Nernstian) relationship to the peak $[K^+]_o$ shifts, and, as already discussed, the *I–V* characteristics of the late GDPSC (and of the glial responses; see Fig. 11) are consistent with a delayed, $[K^+]_o$-mediated effect. Formally, the *I–V* characteristics of a K^+-evoked depolarizing current (I_K) can be derived easily from the Goldman–Hodgkin–Katz constant field current equation:

$$I_K = F^2 R^{-1} T^{-1} V_m P_K \frac{[K^+]_o - [K^+]_i e^{kV_m}}{1 - e^{kV_m}}, \tag{1}$$

where $k = FR^{-1}T^{-1}$, $[K^+]_i$ is the intracellular K^+ concentration, and V_m, P_K, F, R, and T have their usual meaning. The dependence of I_K on $[K^+]_o$ is obtained by differentiation with respect to $[K^+]_o$. Assuming that the cell is under voltage clamp,

$$\frac{\partial I_K}{\partial [K^+]_o} = F^2 R^{-1} T^{-1} P_K \frac{V_m}{1 - e^{kV_m}}. \tag{2}$$

Because $V_m/(1 - e^{kV_m})$ is always negative, $\partial I_K/\partial [K^+]_o$ is also negative at any V_m; i.e., a rise in $[K^+]_o$ causes an inward current at any V_m. In addition, $V_m/(1 - e^{kV_m})$ approaches asymptotically zero at positive values of V_m.

Strongly depolarizing GABAergic postsynaptic responses are associated with certain kinds of long-term changes in synaptic efficacy (Collin et al., 1995), in the generation of epileptiform activity (Taira et al., 1997) (see also Stasheff et al., 1993), and in the immature nervous system (Cherubini et al., 1991). It will be interesting to see in future work whether, and to what extent, activity-induced $[K^+]_o$ shifts are involved in the diverse phenomena that involve long-lasting GABAergic depolarizing responses in the developing and mature brain. Information on excitatory $GABA_A$ receptor-mediated responses is also likely to shed light on the mechanisms of functional coupling within the inhibitory interneuronal network and of its oscillatory properties (cf. Michelson and Wong, 1994; Whittington et al., 1995; Traub et al., 1996; Lamsa and Kaila, 1997).

REFERENCES

Aram JA, Michelson HB, Wong RKS (1991) Synchronized GABAergic IPSPs recorded in the neocortex after blockade of synaptic transmission mediated by excitatory amino acids. J Neurophysiol 65:1034–1041.

Avoli M, Louvel J, Kurcewicz I, Pumain R, Barbarosie M (1996) Extracellular free potassium and calcium during synchronous activity induced by 4-aminopyridine in the juvenile rat hippocampus. J Physiol (Lond) 493:707–717.

Barolet AW, Morris ME (1991) Changes in extracellular K^+ evoked by GABA, THIP, and baclofen in the guinea-pig hippocampal slice. Exp Brain Res 84:591–598.

Benos DJ (1982) Amiloride: a molecular probe of sodium transport in tissues and cells. Am J Physiol 242:C131–C145.

Bevensee MO, Cummins TR, Haddad GG, Boron WF, Boyarski G (1996) pH regulation in single CA1 neurons acutely isolated from the hippocampi of immature and mature rats. J Physiol (Lond) 494:315–328.

Blanton MG, Loturco JJ, Kriegstein AR (1989) Whole cell recording from neurons in slices of reptilian and mammalian cerebral cortex. J Neurosci Methods 30:203–210.

Bormann J, Hamill OP, Sakmann B (1987) Mechanism of anion permeation through channels gated by glycine and γ-aminobutyric acid in mouse cultured spinal neurones. J Physiol (Lond) 385:243–286.

Cherubini E, Gaiarsa JL, Ben-Ari Y (1991) GABA: an excitatory transmitter in early postnatal life. Trends Neurosci 14:515–519.

Chesler M, Kaila K (1992) Modulation of pH by neuronal activity. Trends Neurosci 15:396–402.

Cole AE, Nicoll RA (1984) Characterization of a slow cholinergic postsynaptic potential recorded *in vitro* from rat hippocampal pyramidal cells. J Physiol (Lond) 352:173–188.

Collin C, Devane WA, Dahl D, Lee C-J, Axelrod J, Alkon DL (1995) Long-term synaptic transformation of hippocampal CA1 γ-aminobutyric acid synapses and the effect of anandamide. Proc Natl Acad Sci USA 92:10167–10171.

Davies CH, Collingridge GL (1993) The physiological regulation of synaptic inhibition by $GABA_B$ autoreceptors in rat hippocampus. J Physiol (Lond) 472:245–265.

Fatima-Shad K, Barry PH (1993) Anion permeation in GABA- and glycine-gated channels of mammalian cultured hippocampal neurons. Proc R Soc Lond [Biol] 253:69–75.

Grover LM, Lambert NA, Schwartzkroin PA, Teyler TJ (1993) Role of HCO_3^- ions in depolarizing $GABA_A$ receptor-mediated responses in pyramidal cells of rat hippocampus. J Neurophysiol 69:1541–1555.

Hille B (1992) Ionic currents of excitable membranes, 2nd Ed. Sunderland, MA: Sinauer.

Jensen MS, Cherubini E, Yaari Y (1993) Opponent effects of potassium on GABA$_A$-mediated postsynaptic inhibition in the rat hippocampus. J Neurophysiol 69:764–771.

Kaila K (1994) Ionic basis of GABA$_A$ receptor channel function in the nervous system. Prog Neurobiol 42:489–537.

Kaila K, Voipio J (1987) Postsynaptic fall in intracellular pH induced by GABA-activated bicarbonate conductance. Nature 330:163–165.

Kaila K, Voipio J (1990) GABA-activated bicarbonate conductance: influence on E_{GABA} and on postsynaptic pH regulation. In: Chloride channels and carriers in nerve, muscle and glial cells (Alvarez-Leefmans FJ, Russell JM, eds), pp 331–353. New York: Plenum.

Kaila K, Pasternack M, Saarikoski J, Voipio J (1989) Influence of GABA-gated bicarbonate conductance on membrane potential, current, and intracellular chloride in crayfish muscle fibres. J Physiol (Lond) 416:161–181.

Kaila K, Paalasmaa P, Taira T, Voipio J (1992) pH transients due to monosynaptic activation of GABA$_A$ receptors in rat hippocampal slices. NeuroReport 3:105–108.

Kaila K, Voipio J, Paalasmaa P, Pasternack M, Deisz RA (1993) The role of bicarbonate in GABA$_A$ receptor-mediated IPSPs in rat neocortical neurons. J Physiol (Lond) 464:273–289.

Kaila K, Smirnov S, Taira T, Voipio J (1995) Both anionic and cationic mechanisms contribute to GABA$_A$ receptor-mediated depolarizing synaptic responses in CA1 pyramidal neurons. Soc Neurosci Abstr 21:244.4.

Lambert N, Grover L (1995) The mechanism of biphasic GABA responses. Science 269:928–929.

Lamsa K, Kaila K (1997) Ionic mechanisms of spontaneous GABAergic events in rat hippocampal slices exposed to 4-aminopyridine. J Neurophysiol, in press.

Lothman EW, Somjen GG (1975) Extracellular potassium activity, intracellular and extracellular potential responses in the spinal cord. J Physiol (Lond) 252:115–136.

Maren TH (1977) Use of inhibitors in physiological studies of carbonic anhydrase. Am J Physiol 232:F291–F297.

Michelson HB, Wong RKS (1994) Synchronization of inhibitory neurones in the guinea-pig hippocampus *in vitro*. J Physiol (Lond) 477:35–45.

Nathan T, Jensen MS, Lambert JDC (1990) The slow inhibitory postsynaptic potential in rat hippocampal neurons is blocked by intracellular injection of QX-314. Neurosci Lett 110:309–313.

Nicoll RA, Malenka RC, Kauer JA (1990) Functional comparison of neurotransmitter receptor subtypes in mammalian central nervous system. Physiol Rev 70:513–565.

Pasternack M, Voipio J, Kaila K (1993) Intracellular carbonic anhydrase activity and its role in GABA-induced acid transients in isolated rat hippocampal pyramidal neurones. Acta Physiol Scand 148:229–231.

Payne JA, Stevenson TJ, Donaldson LF (1996) Molecular characterization of a putative K-Cl cotransporter in rat brain. J Biol Chem 271:16247–16252.

Perkins KL, Wong RKS (1996) Ionic basis of the postsynaptic depolarizing GABA response in hippocampal pyramidal cells. J Neurophysiol 76:3886–3894.

Perreault P, Avoli M (1992) 4-Aminopyridine-induced epileptiform activity and a GABA-mediated long-lasting depolarization in the rat hippocampus. J Neurosci 12:104–115.

Raley-Susman KM, Sapolsky RM, Kopito RR (1993) Cl$^-$/HCO$_3^-$ exchange function differs in adult and fetal rat hippocampal neurons. Brain Res 614:308–314.

Schwiening CJ, Boron WF (1994) Regulation of intracellular pH in pyramidal neurones from the rat hippocampus by Na$^+$-dependent Cl$^-$-HCO$_3^-$ exchange. J Physiol (Lond) 475:59–67.

Staley KJ, Otis TS, Mody I (1992) Membrane properties of dentate gyrus granule cells: comparison of sharp microelectrode and whole-cell recordings. J Neurophysiol 67:1346–1358.

Staley KJ, Soldo BL, Proctor WR (1995) Ionic mechanisms of neuronal excitation by inhibitory GABA$_A$ receptors. Science 269:977–981.

Stasheff SF, Mott DD, Wilson WA (1993) Axon terminal hyperexcitability associated with epileptogenesis *in vitro*. II. Pharmacological regulation by NMDA and GABA$_A$ receptors. J Neurophysiol 70:976–984.

Taira T, Paalasmaa P, Voipio J, Kaila K (1995) Relative contributions of excitatory and inhibitory neuronal activity to alkaline transients evoked by stimulation of Schaffer collaterals in the rat hippocampal slice. J Neurophysiol 74:643–649.

Taira T, Lamsa K, Kaila K (1997) Post-tetanic excitation mediated by GABA$_A$ receptors in rat CA1 pyramidal neurons. J Neurophysiol 77:2213–2218.

Tang C-M, Presser F, Morad M (1988) Amiloride selectively blocks the low threshold (T) calcium channel. Science 240:213–215.

Thompson SM, Gähwiler BH (1989a) Activity-dependent disinhibition. II. Effects of extracellular potassium, furosemide, and membrane potential on E$_{Cl^-}$ in hippocampal CA3 neurons. J Neurophysiol 61:512–523.

Thompson SM, Gähwiler BH (1989b) Activity-dependent disinhibition. I. Repetitive stimulation reduces IPSP driving force and conductance in the hippocampus *in vitro*. J Neurophysiol 61:501–511.

Thompson SM, Deisz RA, Prince DA (1988a) Outward chloride/cation co-transport in mammalian cortical neurons. Neurosci Lett 89:49–54.

Thompson SM, Deisz RA, Prince DA (1988b) Relative contributions of passive equilibrium and active transport to the distribution of chloride in mammalian cortical neurons. J Neurophysiol 60:105–124.

Traub RD, Whittington MA, Colling SB, Buzsaki G, Jefferys JGR (1996) Analysis of gamma rhythms in the rat hippocampus *in vitro* and *in vivo*. J Physiol (Lond) 493:471–484.

Voipio J, Kaila K (1993) Interstitial PCO$_2$ and pH in rat hippocampal slices measured by means of a novel fast CO$_2$/H$^+$-sensitive microelectrode based on a PVC-gelled membrane. Pflügers Arch 423:193–201.

Voipio J, Pasternack M, MacLeod K (1994) Ion-sensitive microelectrodes. In: Microelectrode techniques, the Plymouth workshop handbook, 2nd Ed (Ogden D, ed), pp 275–316. Cambridge, UK: The Company of Biologists.

Voipio J, Paalasmaa P, Taira T, Kaila K (1995) Pharmacological characterization of interstitial pH transients evoked by selective synaptic and exogenous activation of AMPA, NMDA, and GABA$_A$ receptors in the rat hippocampal slice. J Neurophysiol 74:633–642.

Voipio J, Lamsa K, Autere A-M, Smirnov S, Taira T, Kaila K (1996) Rise in extracellular K$^+$ and fall in Ca^{2+} induced by tetanic stimulation of inhibitory interneurons in area CA1 of rat hippocampal slices. Soc Neurosci Abstr 22:314.2.

Whittington MA, Traub RD, Jefferys JGR (1995) Synchronized oscillations in interneuron networks driven by metabotropic glutamate receptor activation. Nature 373:612–615.

Wong RKS, Watkins DJ (1982) Cellular factors influencing GABA response in hippocampal pyramidal cells. J Neurophysiol 48:938–951.